IEEE Access
Multidisciplinary | Rapid Review | Open Access Journal

Received October 6, 2020, accepted October 21, 2020, date of publication October 23, 2020, date of current version November 3, 2020.

Digital Object Identifier 10.1109/ACCESS.2020.3033472

Assessing the Quality of Wearable EEG Systems Using Functional Connectivity

YACINE MAHDID[1], UNCHEOL LEE[2], AND STEFANIE BLAIN-MORAES[3]
[1]Integrated Program in Neuroscience, McGill University, Montreal, QC H3G 1Y5, Canada
[2]Department of Anesthesiology, University of Michigan, Ann Arbor, MI 48105, USA
[3]School of Physical and Occupational Therapy, McGill University, Montreal, QC H3G 1Y5, Canada

Corresponding author: Stefanie Blain-Moraes (stefanie.blain-moraes@mcgill.ca)

This work was supported by the Natural Science and Engineering Research Council of Canada under Grant RGPIN-2016-03817.

ABSTRACT Assessing the data quality of wearable electroencephalogram (EEG) systems is critical to collecting reliable neurophysiological data in non-laboratory environments. To date, measures of signal quality and spectral characteristics have been used to characterize wearable EEG systems. We demonstrate that these traditional measures do not provide fine-grained differentiation between the performance of four popular wearable EEG systems (the Epoc+, OpenBCI, DSI-24 and Quick-30 Dry EEG). Using two computationally inexpensive metrics of undirected functional connectivity (phase lag index) and directed functional connectivity (directed phase lag index), we compare the integrity of the phase relationships captured by wearable systems to those recorded from a high-density research-grade EEG system (Electrical Geodesics Inc). Our results demonstrate that functional connectivity analyses provide additional discriminatory information about wearable EEG systems, with clear differentiation of the cosine similarity between research-grade functional connectivity patterns and those generated by each wearable system. We provide a freely available Matlab toolbox containing all metrics described in this paper such that researchers and non-experts interested in wearable EEG systems can easily assess the quality of systems not characterized in this study, thus advancing the translation of EEG research into non-laboratory settings.

INDEX TERMS Electroencephalography, functional connectivity, wearable technology.

I. INTRODUCTION

Effective translational research requires collecting high-quality neurophysiological data in non-laboratory settings. Electroencephalography (EEG) uses non-invasive scalp electrodes to measure the electrical activity of cerebral cortical neurons, and is a popular method of collecting neurophysiological data due to its relative accessibility and low cost compared to other neuroimaging technologies (e.g. functional magnetic resonance imaging (fMRI); magnetoencephalography (MEG)). Although EEG is typically recorded by sophisticated medical instruments operated by professionally trained experts, there has been a recent proliferation of portable and affordable single- and multi-channel EEG devices marketed for personal and everyday applications [1]–[6]. These devices – referred to as consumer-grade EEG, mobile EEG, translational EEG and wearable EEG – have become increasingly popular due to their low cost, their ease of setup and their relatively acceptable performance [7]. To date, they have been used in applications ranging from clinical monitoring (e.g. epilepsy [8]); assistive technologies (e.g. brain-computer interfaces [9]); and monitoring the mental state of workers [10], drivers [11], and athletes [12].

As EEG signals are weak and prone to noise, obtaining high quality EEG data is a common challenge. Medical and research groups have extensively tested the quality of wearable EEG systems (e.g. [13]–[16]). These devices are typically compared to research-grade EEG equipment on the basis of 1) EEG signal quality; 2) spectral properties of continuous EEG recordings; and/or 3) the detection of event-related potentials (ERPs). EEG signal quality is typically assessed by the percentage of artifact-contaminated EEG, and the signal-to-noise ratio of the collected data [16]–[20]. Spectral properties are evaluated in relation to established phenomena, such as the Berger effect, and band power variation in relation to various tasks [14], [17], [18], [20], [21]. The ability to detect ERPs in various environments is

The associate editor coordinating the review of this manuscript and approving it for publication was Praveen Gunturi.

another common metric of the quality of a mobile EEG system [14]–[16], [19], [21]–[23].

These traditional comparison metrics for wearable EEG systems have their roots in the neuroscientific concepts of functional segregation and the localization of function in the brain. However, since studies of patients with brain lesions led to the refutation of localization as a complete or sufficient account of cortical organization, neuroscientific studies have shifted their focus to functional integration and connectivity, with the annual increase in publications on connectivity surpassing the year increase in publications on activation in 2011 [24]. While the application of functional connectivity metrics to EEG data has become increasingly popular, the quality of wearable EEG systems has never been evaluated according to these metrics. The motivation for this paper was to develop the infrastructure to enable non-experts to assess the quality of wearable EEG systems with respect to measures of functional connectivity.

The remainder of the paper is structured as follows: we briefly present the background of functional connectivity in Section II. The description of the four wearable EEG systems, the research-grade EEG system and the details of data acquisition and analysis are presented in Section III. Section IV compares the four wearable EEG systems against traditional research-grade equipment using signal quality, spectral measures and functional connectivity measures. Sections V and VI conclude the paper with observations/discussion, conclusions and directions for future work. This paper also provides a freely available Matlab toolbox containing these measures, which can be effectively used to assess the quality of wearable EEG systems.

II. FUNCTIONAL CONNECTIVITY

Functional connectivity has become a powerful tool for assessing neural phenomenon such as conscious awareness [25]–[28], and has been used to characterize both neural dysfunction [29], [30] as well as state transitions in the brain [31], [32]. Functional connectivity measures statistical dependences among remote neurophysiological events [24] and can be directed or undirected. Undirected functional connectivity is calculated from phase coupling of band-limited oscillatory signals, or from coupled aperiodic fluctuations of signal envelopes [33]. Common examples of techniques used to assess undirected functional connectivity (dependencies) include various measures of synchrony, correlation and coherence [34]. Directed functional connectivity metrics consider the temporal precedence of two signals. Prime examples of directed functional connectivity include partial directed coherence [35], directed transfer functions [36], Granger causality [37], symbolic transfer entropy [38], and directed phase lag index [39].

Of particular interest to the field of wearable EEG systems are the measures of phase lag index (PLI) and directed phase lag index (dPLI) due to their robustness against volume conduction and their low computational cost, which makes them amenable to real-time calculation in a wearable system. Moreover, PLI and dPLI have successfully been used to characterize brain network properties with significant clinical implications, including loss and recovery of consciousness [27], [31], [40] and delirium [41], and to identify network-level changes in conditions such as autism [42], dementia [43] and fragile X syndrome [44].

To date, wearable EEG systems have been evaluated based on metrics examining local EEG features, rather than on EEG connectivity features. As functional connectivity – by definition – measures the statistical dependencies between two electrodes, this metric is only applicable to multi-sensor, rather than single-point sensor, systems. In this paper, we select four multi-channel, wearable EEG headsets that represent a range of cost, electrode coverage and ease of setup, and compare their ability to reproduce the functional connectivity patterns of a research-grade EEG system.

III. METHODS

A. ELECTROENCEPHALOGRAPHY DATA ACQUISITION, PRE-PROCESSING AND ANALYSIS

An overview of EEG data acquisition, pre-processing and analysis are presented in Figure 1. EEG data were acquired from one research-grade headset and four wearable headsets (Table 1). We considered an EEG system to be wearable if it was mobile and wireless, enabling EEG to be recorded outside of the laboratory [16]; and a research-grade system a high-density, wired EEG system, widely used in research studies. All systems were setup according to their respective best practices (e.g. acceptable levels of impedance), detailed below.

Headset 1: 128-channel HydroCel Geodesic Sensor Net from Electrical Geodesics Inc. (EGI). The electrode net was soaked in a solution of potassium chloride and baby shampoo for 10 minutes prior to application. The electrode net was landmarked to Cz, and impedances were reduced to below 50 kΩ prior to data recording. All channels were referenced to Cz, and data was collected at a sampling rate of 500 Hz.

Headset 2: Quick-30 from Cognionics. The 30 dry electrodes in this headset did not require any preparation prior to application. Electrode impedance was reduced to below 1 MΩ by removing the hair from under the electrodes and gentle abrasion of the scalp prior to data recording. All channels were reference to A2 and sampled at 500 Hz.

Headset 3: DSI-24 from Wearable Sensing. The 24 dry electrodes in this headset were mounted on articulating bearings that maximized contact against the scalp. The electrode impedances were reduced to below 1 MΩ using a special tool that parted the hair around and below the electrodes. All channels were referenced to Pz and data was sampled at a frequency of 300 Hz.

Headset 4: EPOC+ from Emotiv. Electrode sponges from all 14 channels were soaked in Ag/AgCl saline solution for 10 minutes prior data collection. Impedances were reduced to below 20 kΩ by parting the hair and moving the electrodes to make good contact with the scalp. All channels were referenced to P3/P4 and data were sampled at 256 Hz.

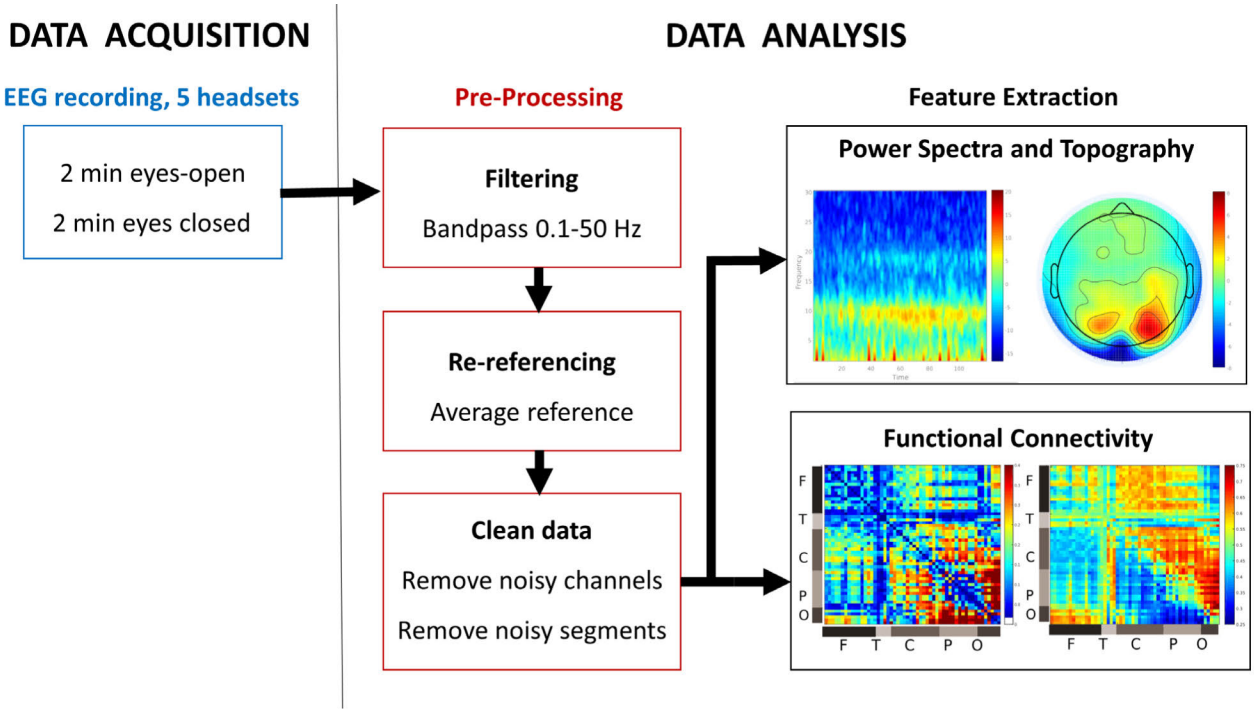

FIGURE 1. Overview of the electroencephalography (EEG) data acquisition and data analysis pipeline.

TABLE 1. EEG acquisition systems specifications.

Headset	Number of Channels	Type of system
Geodesic Sensor Net (Electrical Geodsics Inc.)	99 (only scalp electrodes retained) (F = 29; T = 10; C = 27; P = 22; O = 11)	Wet
Quick-30 (Cognionics)	30 (F = 11; T = 2; C = 5; P = 5; O = 6)	Dry
DSI – 24 (Wearable Sensing)	21 (F = 7; T = 2; C = 3; P = 5; O = 2)	Dry
EPOC + (EMOTIV)	14 (F = 8; T= 2; C = 0; P = 2; O = 2)	Wet
Cyton Board (OpenBCI)	8 (F = 3; P= 3; O = 2)	Dry

Headset 5: Ultracortex "Mark IV" EEG Headset with Cyton Biosensing Board (8-channel) from Open BCI. The 8-channel system was composed of a Cyton 8-channel Biosensing Board, and a 3D printed headset which secured Dry Comb Electrodes. The system was fabricated and assembled according to instructions on the OpenBCI website (http://docs.openbci.com). It was not possible to measure electrode impedance; thus, signal quality of each channel was assessed through visual inspection, and electrode positions were adjusted to maximize signal quality. Data were referenced to A2 and sampled at 250 Hz.

After data collection, the EEG was bandpass filtered using a finite impulse response filter between 0.1 and 50 Hz and re-reference to an average reference. All segments of data containing noise or non-physiological artifacts were identified by an investigator experienced in reading electroencephalograms and removed in EEGlab. Segments containing excessive sweat artefact (i.e. more than 2 standard deviations away from the mean) that persisted over 5 seconds were removed from the data. Segments containing high frequency electromyogram (EMG) artefacts were also removed from the data. Channels that did not record reliable EEG data (e.g. due to poor contact with the scalp) were identified through visual inspection of the waveforms and channel-specific spectrogram and removed from the data. Electrooculogram (EOG) artefact was not removed from the EEG data from any headset; while techniques such as independent component analysis (ICA) would have effectively removed this artefact,

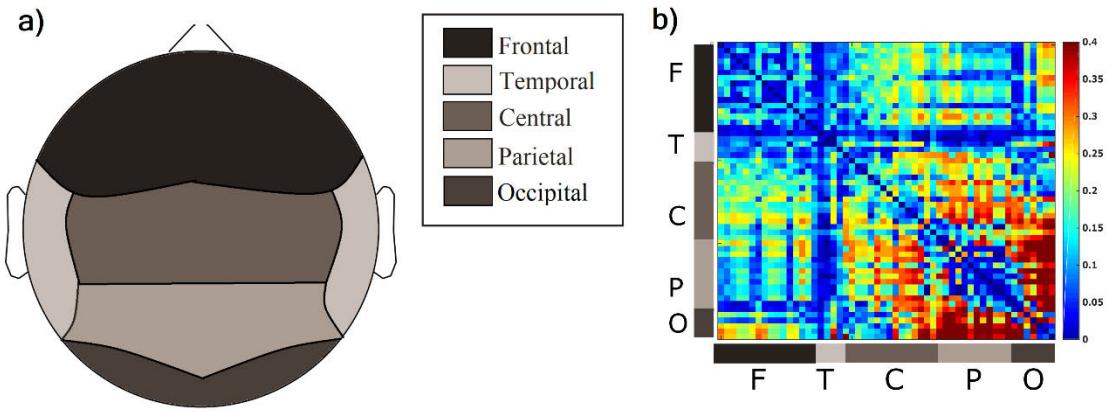

FIGURE 2. Functional connectivity schematic. a) Segmentation of the head for visualization of functional connectivity between all combinations of electrodes. For each headset, electrodes were categorized as frontal (F), temporal (T), central (C), parietal (P) or occipital (O) according to the International 10-20 system. b) Example left-hemisphere PLI matrix, generated using data from gold-standard system. The channels within each region are organized centrally to laterally, beginning at the anterior-most part of the region and following to the posterior-most part.

they are more effective on headsets with a greater number of channels, and this pre-processing step would have biased the subsequent analysis towards higher-density systems. The cleaned EEG was then analyzed using EEGapp, a freely available Matlab toolbox (www.github.com/BIAPT/EEGapp).

1) SPECTRAL AND TOPOGRAPHIC ANALYSIS

Spectrograms were computed between 1-30 Hz using the multitaper method, with window lengths of $T = 2$ s, step size of 0.1 s, time-bandwidth product $NW = 2$, number of tapers $K = 3$. Electroencephalographic data from all available channels were used in the analysis. Scalp power distributions at 10 Hz – the subject's peak alpha frequency - were also calculated across the average spectrogram using the topoplot function in EEGlab [45].

2) FUNCTIONAL CONNECTIVITY ANALYSIS

Functional connectivity between all combinations of electrode pairs was assessed using phase lag index (PLI) and directed phase-lag index (dPLI). These metrics were chosen over other measures of functional connectivity such as coherence, as they are sensitive only to nonzero phase lead/lag relationships, and thus reduce the problem of volume conduction [46]. The instantaneous phase of each channel of the EEG was extracted using a Hilbert transform, and phase difference $\varphi_t t$ was calculated between channels, where $\Delta\varphi_t = \varphi_{i,t} - \varphi_{j,t}$, t = 1, 2, . . . , n, where n is the number of samples in one epoch and i and j included all channels in the EEG headset. PLI was then calculated as follows:

$$PLI_{ij} = \lceil \langle sign(\Delta\varphi_t) \rangle \rceil$$

Here, the sign() function results in 1 if $\Delta\varphi_t > 0$, 0 if $\Delta\varphi_t = 0$, and -1 if $\Delta\varphi_t < 0$. Thus, a PLI value close to 1 indicates that the instantaneous phase of one signal is consistently ahead of another, and the phases are locked, whereas a PLI value close to 0 indicates no consistent phase lead or lag relationship between channels. The direction of the phase-lead/lag relationship between channels i and j were calculated using dPLI [39].

$$dPLI_{ij} = \langle H(\Delta\pi_t) \rangle$$

Here, $H(x)$ represents the Heaviside step function, where $H(x) = 1$ if $x > 0$, $H(x) = 0.5$ if $x = 0$ and $H(x) = 0$ otherwise. Thus, if on average signal i leads signals j, dPLI will be between 0.5 and 1, and if signal j leads signal i, dPLI will be between 0 and 0.5. If there is no phase-lead/phase-lag relationship between signals, dPLI = 0.5.

To quantify the effects of spurious phase relationships, surrogate datasets were calculated as follows. The phase time series of channel i was maintained, while in channel j, the phase time series from 0 to x was changed with the phase time series from x to n, where n is the number of samples in one epoch, and $0 < x < n$. Thus, existing phase relationships were eliminated while maintaining the spectral properties of each condition. The data were permutated 20 times, and PLI and dPLI values were corrected by subtracting the mean of the surrogate dataset.

Functional connectivity was calculated across delta (1-4 Hz); theta (4-8 Hz); alpha (8-13 Hz) and beta (13-30 Hz) frequency bands. As the functional connectivity within both hemispheres of the brain were symmetric, PLI and dPLI results are only presented for the left hemisphere, according to the schematic illustrated in Figure 2.

3) COMPARISON OF WEARABLE SYSTEM TO THE GOLD STANDARD

The frequency of the dominant power peaks in each spectrogram were compared between wearable systems and the gold standard system. Topographic maps were compared based on the location of the dominant power across brain regions.

To compare the functional connectivity patterns between devices, the number of channels in the high-density system

was reduced to match the number of channels and channel locations of each of the wearable headsets. Each wearable headset was aligned to the gold standard system by matching all electrodes with 10-20 labels (e.g. Fz, C3, P4) to their corresponding counterparts. For all electrodes without a 10-20 label, the Euclidean distance to all nearest neighbours of the gold-standard headset was calculated using EGI's default 3D electrode location position file. The electrodes in the high-density system with the shortest distance to the electrode in each of the wearable systems were selected to generate comparative functional connectivity data.

The PLI and dPLI matrices were compared against the gold standard using cosine similarity, defined as:

$$s = \frac{\boldsymbol{b_i} \cdot \boldsymbol{b_j}}{\|\boldsymbol{b_i}\| \|\boldsymbol{b_j}\|}$$

where b_i and b_j are the connectivity values for the wearable headset (i) and the gold standard headset (j) [47]. Cosine similarity ranges from -1 to 1, where 1 indicates identical functional connectivity patterns between headsets, -1 indicates diametrically opposite functional connectivity patterns between headsets, and 0 indicates orthogonality or decorrelation.

B. CASE EXAMPLE

The added value of functional connectivity in assessing wearable EEG systems was demonstrated in a case example of a single participant ($n = 1$) (male, 24 years) using the four wearable systems and the research-grade system. Continuous EEG was recorded in two 2-minute blocks: 1) eyes-closed rest; and 2) eyes-open rest. Data collected from each headset were compared using spectral, topographic and functional connectivity analyses. Data from each headset were segmented into non-overlapping 10-second epochs, and functional connectivity was calculated for each frequency band, for each epoch. Average functional connectivity for each state was generated by averaging connectivity across all epochs.

To establish how representative these single block recordings were of headset performance across sessions, we also collected 10 sessions of eyes-closed rest and eyes-open rest from the same subject across five different days, at various times of day (i.e. morning, afternoon and evening) for two EEG systems. The three EEG analysis metrics were averaged across the ten sessions, and the average spectrogram, topographic maps and functional connectivity matrices were compared to those computed for the single block recording.

IV. RESULTS

A. TRADITIONAL QUALITY METRICS DO NOT DIFFERENTIATE BETWEEN WEARABLE EEG SYSTEMS

The percentage of artifact-contaminated EEG and the spectral properties of continuous EEG recordings are traditionally used to assess the quality of wearable EEG systems. Of the four wearable EEG systems tested in this study, poor signal quality affected data recorded from two headsets: the Quick-30 (3 channels) and the EPOC+ (2 channels). These channels were eliminated from subsequent analysis (Figure 3a). Spectral analysis demonstrated that all systems were able to detect the Berger effect - an increase in alpha power in the eyes-closed condition (Figure 3b), while one wearable system (the EPOC+) was unable to detect the posterior dominant rhythm at 10 Hz in parietal and occipital regions (Figure 3c). Cumulatively, while these quality metrics reveal the limitations of several systems, they do not provide a fine-grained differentiation between performance of wearable EEG headsets.

B. FUNCTIONAL CONNECTIVITY PATTERNS EFFECTIVELY DISTINGUISH THE QUALITY OF WEARABLE EEG SYSTEMS

Functional connectivity and directed functional connectivity patterns were calculated across delta, theta, alpha and beta bandwidths. In this section, we focus on comparing the functional connectivity patterns in the alpha bandwidth, which has been strongly linked to cognitive functioning [48] and conscious awareness [31], [49]. Functional connectivity patterns in delta, theta and beta are presented in the Supplementary Material (Figures S1-S3). While the nuanced comparisons between wearable headsets and the gold standard headset differ across bandwidths, the conclusions that can be drawn about the quality of each wearable headset are consistent with those in the alpha bandwidth.

The functional connectivity patterns generated from the research-grade EEG system were used as the gold standard against which the wearable headset patterns were compared. As expected in the research-grade system, posterior regions showed high functional connectivity during the eyes-closed condition, and central regions showed moderate functional connectivity during the eyes-open condition (Figure 4a, left column). A feedback lead/lag relationship dominated in posterior regions (e.g. from central to parietal, from central to occipital) in the eyes-closed condition and was diffusely present in all regions in the eyes-open condition (Figure 4b, left column).

Functional connectivity and directed functional connectivity patterns for each wearable headset are presented in Figure 5 and Figure 6, respectively. The Quick-30 EEG system displayed more frontoparietal and fronto-occiptal functional connectivity than the gold standard in the eyes-closed condition (PLI cosine similarity = 0.68), and was more similar to the gold-standard in the eyes-opened condition (PLI cosine similarity = 0.75). Feedback connectivity was present in anterior regions (c.f. posterior regions in the gold-standard) during the eyes-closed condition (dPLI cosine similarity = 0.84), and was more similar to the gold-standard in eyes-open conditions (dPLI cosine similarity = 0.91) (Figure 3, Quick-30 A versus B).

The DSI-24 EEG system presented higher functional connectivity across all electrode pairs in the eyes-closed condition (PLI cosine similarity = 0.82), but similar patterns in the eyes-open condition (PLI cosine similarity = 0.87).

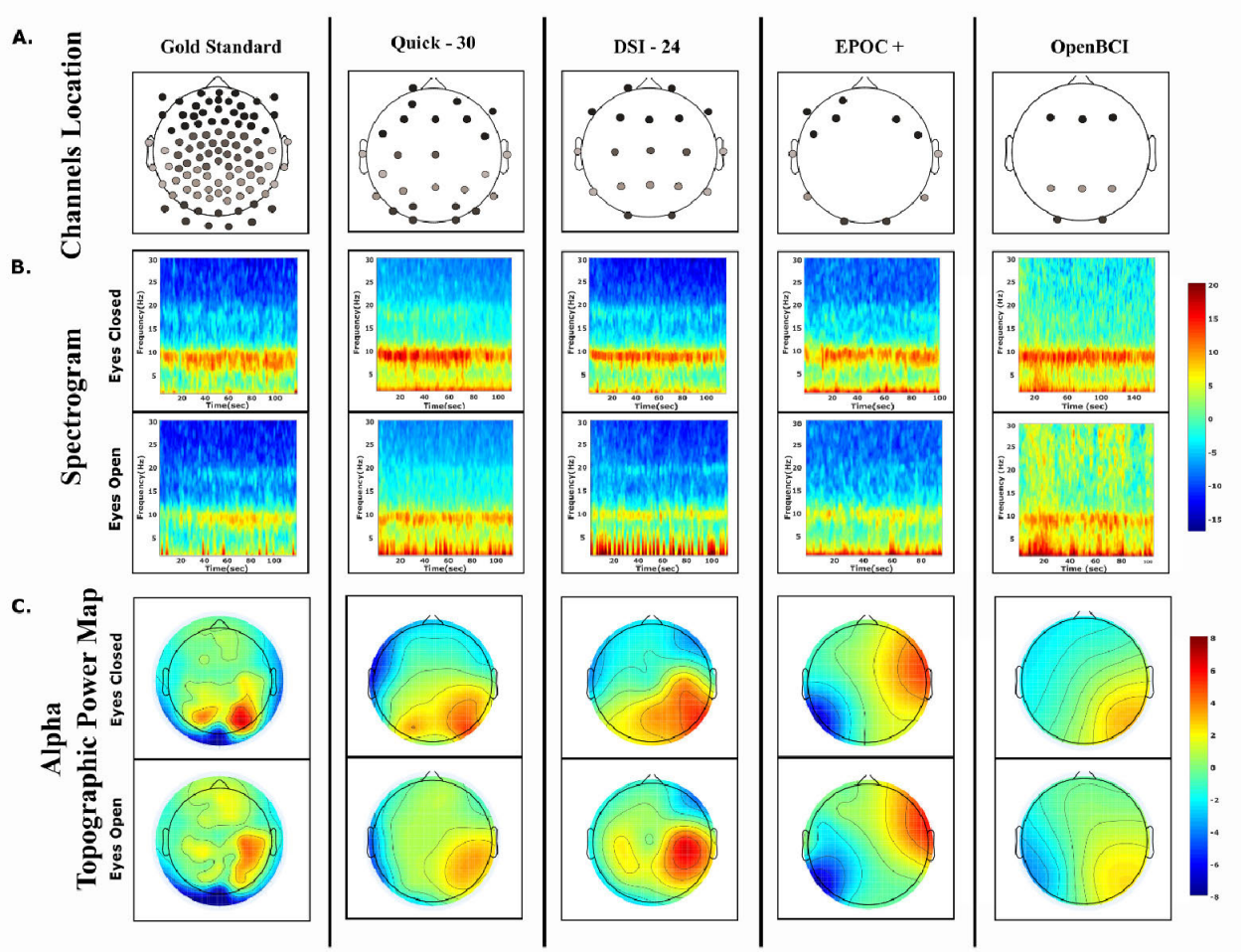

FIGURE 3. Spectral and topographic analysis. Top row: Location of the channels for the Geodesic Sensor Net (i.e. gold standard), Quick-30, DSI-24, EPOC + and OpenBCI. Middle row: Spectrogram across all channels for each EEG system for eyes-closed and eyes-open conditions. Bottom row: Topographic power map at 10 Hz across the average spectrogram for each EEG system under both conditions.

It captured the posterior feedback lead-lag relationship, but also spurious centroparietal lead-lag relationships in the eyes-closed condition (dPLI cosine similarity = 0.85). Lead/lag relationships were near identical to the gold-standard in the eyes-opened condition (dPLI cosine similarity = 0.97) (Figure 3, DSI-24 A versus B).

The EPOC+ EEG system presented spurious functional connectivity in the eyes-closed condition (PLI cosine similarity = 0.85) and was unable to reproduce patterns of the eyes-open condition (PLI cosine similarity = 0.79). While the dPLI cosine similarity was 0.92 in the eyes-closed condition, directed functional connectivity showed patterns opposite of those expected (e.g. feedforward lead-lag relationships), and the eyes-open condition presented random lead/lag patterns (dPLI cosine similarity = 0.75) (Figure 3, EPOC+ A versus B).

The OpenBCI Cyton Dry EEG system produced spurious functional connectivity between the parietal electrode and all other channels under both eyes-closed and open conditions (PLI cosine similarity = 0.62, 0.65, respectively). It did not capture the expected phase lead-lag relationship patterns under either condition (dPLI cosine similarity = 0.79, 0.78, respectively) (Figure 3, OpenBCI A versus B).

While signal quality, spectral analysis and topographic analysis did not differentiate the quality of all four wearable headsets, the results of the functional connectivity analysis provided additional discriminatory information. Across all frequency bands and both eyes-open and eye-closed conditions, the DSI-24 had the highest cosine similarity to the gold standard functional connectivity and directed functional connectivity patterns, followed by the Cognisonics 30 and EPOC+, with the OpenBCI headset presenting the lowest cosine similarity to expected patterns (Figure 7).

C. SINGLE SESSION RECORDINGS ARE REPRESENTATIVE OF AVERAGE PERFORMANCE OF WEARABLE SYSTEMS

Spectrograms, topographic maps and functional connectivity matrices calculated from the EGI high-density system and the DSI-24 were compared between a single session (e.g. one two-minute EEG epoch) and an average of ten 2-minute EEG

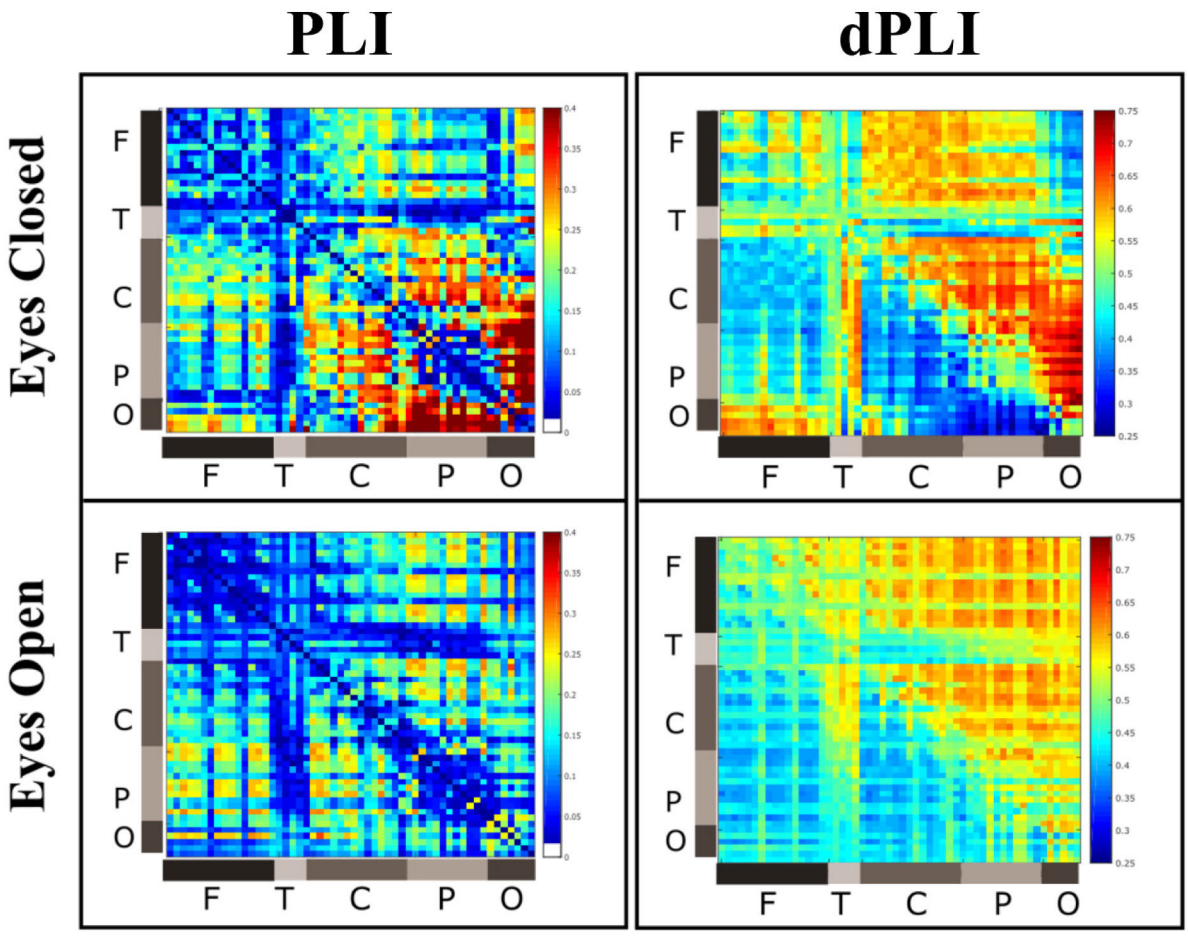

FIGURE 4. Functional connectivity (PLI) and directed functional connectivity (dPLI) matrices from the research-grade EEG system during eyes closed and eyes opened conditions. PLI connectivity is high in posterior regions during the eyes-closed condition; dPLI connectivity demonstrates feedback lead/lag relationships across both conditions. F = frontal; T = temporal; C = central; P = parietal; O = occipital.

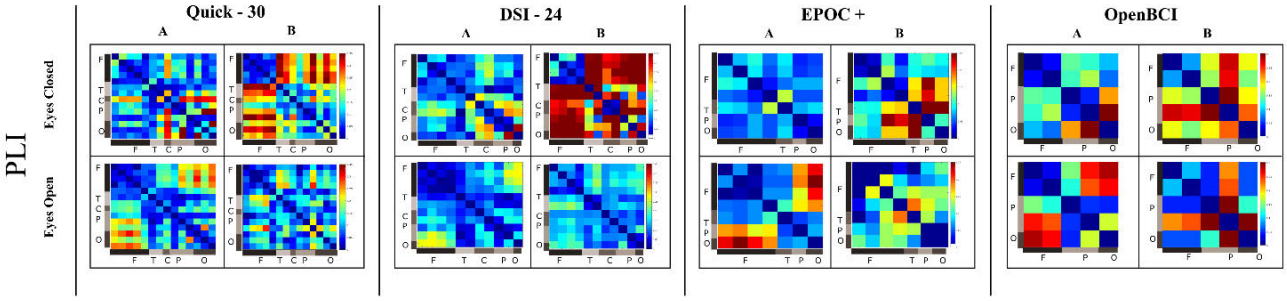

FIGURE 5. Phase lag index (PLI) matrices in the alpha bandwidth across four wearable EEG systems. PLI matrices generated from the corresponding nearest-neighbour electrodes from the research-grade EEG system (column A) are compared against PLI matrices generated from the wearable headset (column B) for eyes closed and eyes opened conditions. F = frontal; C = central; T = temporal; P = parietal; O = occipital.

epochs recorded at various times of the day across 5 different days. The single session functional connectivity data was near identical to the averaged data across both gold standard (PLI cosine similarity = 0.97; dPLI cosine similarity = 0.995) and wearable systems (PLI cosine similarity = 0.991; dPLI cosine similarity = 0.999) (Figure 8). This degree of similarity demonstrates that the comparisons of headset performance based on single session data are representative of the average performance of the wearable systems.

V. DISCUSSION

In this paper, we demonstrate that functional connectivity metrics can provide complementary information to signal quality and spectral measures in assessing the quality of

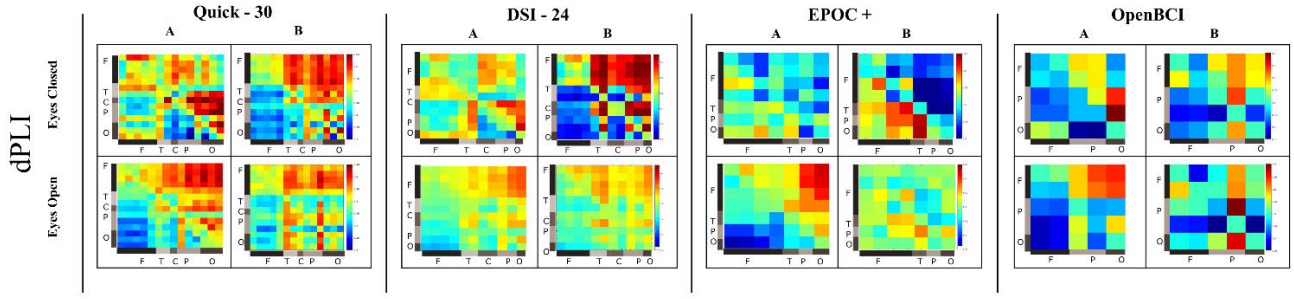

FIGURE 6. Directed phase lag index (dPLI) matrices in the alpha bandwidth across four wearable EEG systems. dPLI matrices generated from the corresponding nearest-neighbour electrodes from the research-grade EEG system (column A) are compared against dPLI matrcies generated for the wearable headset (column B) for eyes closed and eyes opened conditions. F = frontal; C = central; T = temporal; P = parietal; O = occipital.

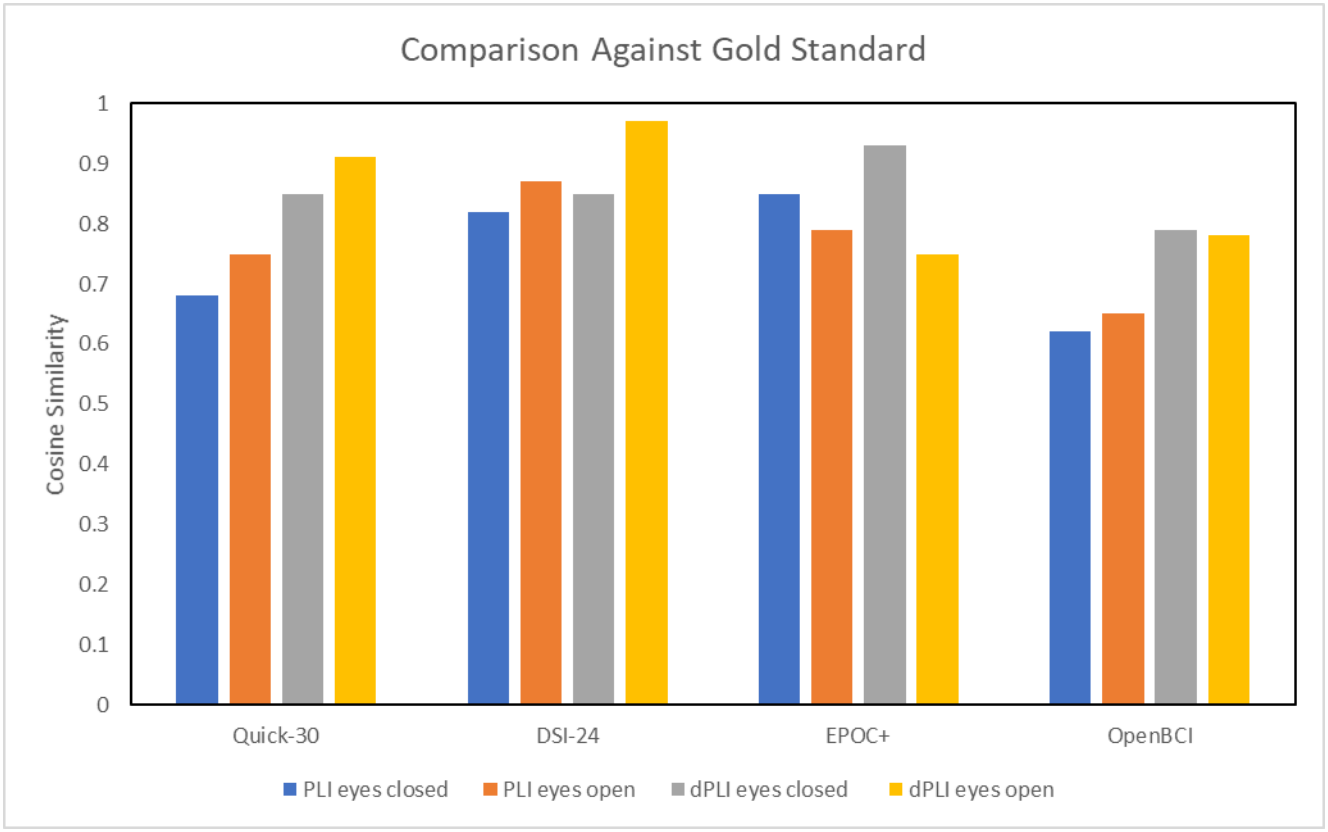

FIGURE 7. Cosine similarity values of phase lag index (PLI) and directed phase lag index (dPLI) calculated from each wearable EEG system compared to the gold standard.

wearable EEG systems. We compared four wearable EEG systems (the Quick-30, DSI-24, EPOC+ and OpenBCI) to a traditional research-grade EEG system from Electrical Geodesics Incorporated. Despite following best practices for setting up the equipment, the Quick-30 and the EPOC+ had several channels with poor signal-to-noise ratios. The quality of the wearable EEG systems could not be further distinguished using spectral nor topographic analysis, with the exception of the EPOC+, whose data resulted in a spurious lateralization of the posterior dominant rhythm [50]. Assessing the systems with functional and directed functional connectivity provided additional information. The OpenBCI system did not produce the expected patterns of functional or directed functional connectivity. The Quick-30 and DSI-24 reproduced expected phase lead/lag relationships and regions of dominant functional connectivity. While both systems were inferior to the gold standard (e.g. exhibiting spurious functional connectivity in the eyes-closed condition), this analysis demonstrated the integrity of the phase data recorded by each headset.

To date, comparisons of wearable EEG headsets to research grade systems have used signal-to-noise ratios,

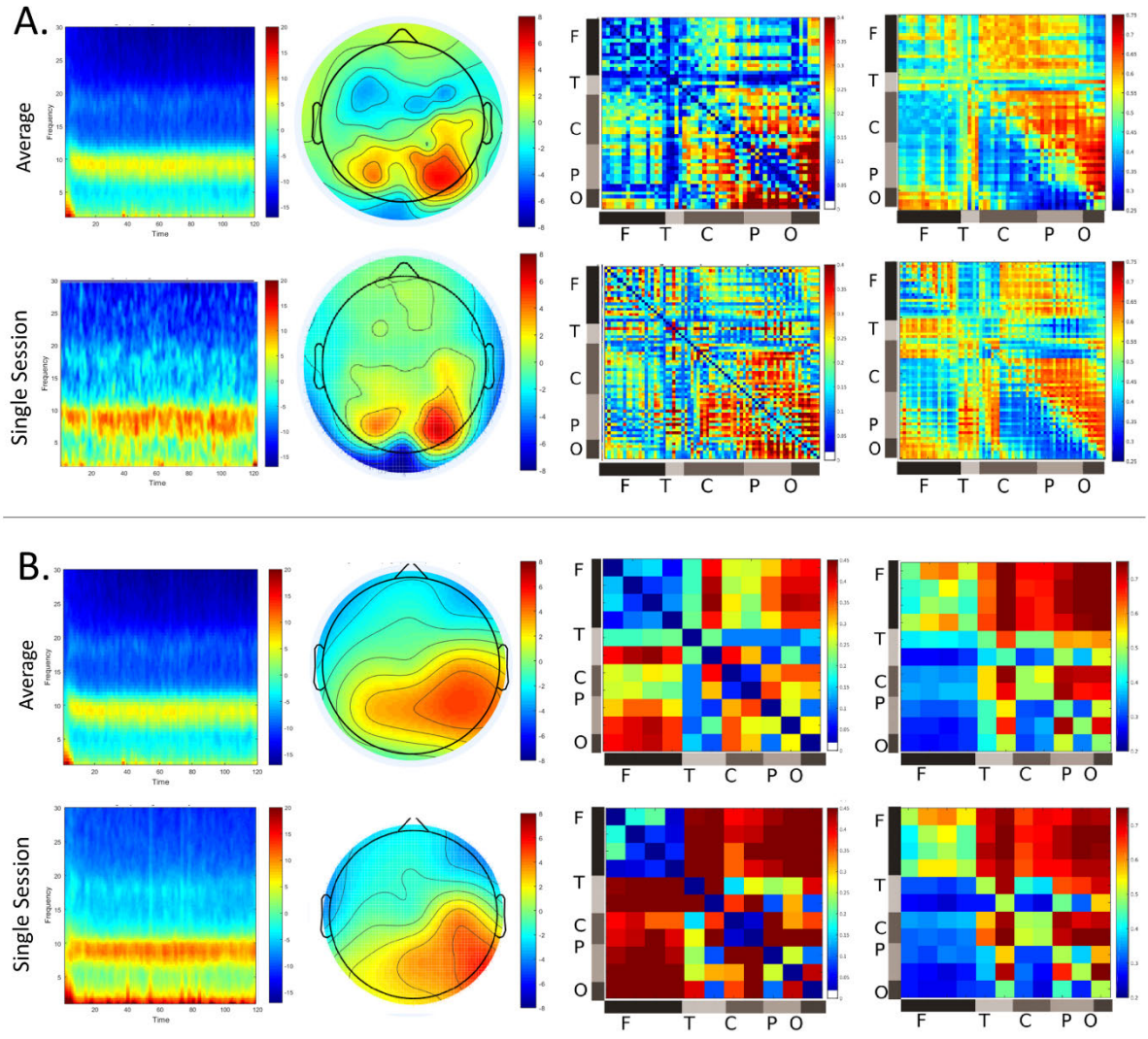

FIGURE 8. Comparison of single session metrics to average metrics generated from 10 sessions recorded over multiple days for (A) research-grade (EGI) and (B) wearable (DSI-24) EEG systems. Spectrograms, topographic maps, phase lag index and directed phase lag index matrices show near identical (e.g. cosine similarity ≥ 0.97) patterns between single session and averaged recordings.

power spectra and topography, as well as event-related potentials as assessment measures. This is the first study to compare wearable EEG headsets on the basis of functional connectivity metrics [14]–[16], [17], [18]–[23]. As measures of functional integration and connectivity become more dominant in the neuroscience literature [24], there is increasing incentive to use these measures on EEG data recorded from translational, wearable headsets. Our analysis demonstrates the feasibility of applying functional connectivity analysis to EEG data collected from select wearable systems. Additionally, our results illustrate that the inclusion of functional connectivity metrics in the comparison of wearable EEG systems provides users with a more nuanced assessment of the quality of these systems. While a direct comparison of our functional connectivity results against other studies is not possible, our signal-to-noise ratio and power spectra and topography results are consistent with other studies, lending credibility to our analysis. In a recent review of ''consumer grade'' EEG systems as research tools, Sawangjai *et al.* reviewed studies from the past five years that used wearable EEG devices as the primary equipment for data collection [7]. Similarly to our findings, reviews of studies that used the Emotiv EPOC+ concluded that data quality, sensor location and electrode number posed considerable challenges when comparing this headset to ''medical grade devices'', while the OpenBCI was more comparable to research grade devices on the basis of signal quality and spectral properties. Our results provide a new dimension for the comparison of these two popular wearable headsets, demonstrating that the functional connectivity patterns were less similar to a research-grade EEG system in the OpenBCI than in the Emotiv EPOC+.

Our demonstration of the added advantages of assessing translational EEG systems with functional connectivity measures need to be interpreted in light of several limitations. First, we evaluated the performance of the headsets on a single-subject basis, as opposed to a group-average. Although this limits the generalizability of our results, we believe that the performance of a wearable EEG system on a subject-by-subject basis is strongly associated with its translational potential. The need for individualization in translational EEG applications has been established, as there is significant heterogeneity in EEG characteristics across the population [51]–[53]. Our case study enables us to compare the quality of the selected EEG headsets on a single-subject level, where idiosyncratic neural patterns – such as our participant's lateralized posterior dominant rhythm – are visible, as opposed to on a group level, where individual patterns are often averaged out. This within-subject comparison highlights the ability for wearable EEG systems to reproduce the subject-specific patterns that are visible in the gold-standard EEG system, providing information that is more relevant to the translational potential of wearable headsets than a between-subject comparison. Second, each headset had a different number and topographic distribution of electrodes. While we accounted for this variability by reducing the gold standard to the nearest-neighbor electrodes for comparison, this may bias the analyses for some headsets. For example, the Emotiv EPOC+ had a sparse distribution of electrodes in posterior brain regions, which skewed the alpha (10 Hz) topographic power map analysis towards frontal regions, in comparison to headsets with a more uniform electrode distribution. Third, we assessed the headsets only on the basis of one measure of functional connectivity (phase lag index) and one measure of directed functional connectivity (directed phase lag index). While these metrics were chosen because of their robustness to volume conduction and their relatively low computational power (i.e. their translational potential), it is possible that other measures of functional connectivity (e.g. envelop-based connectivity metrics, information theory-based connectivity metrics) do not provide the same discriminatory power between headsets. Finally, all headsets were assessed based on continuous rather than event-related EEG metrics. The ability to robustly detect ERPs in various environments has often been used as a marker of quality of mobile EEG headsets; the results presented in this paper provide a complementary assessment to this popular approach and are particularly relevant for translational EEG applications focused on characterizing connectivity patterns in brain networks.

To accompany this article, we developed a freely available open-source Matlab toolbox for spectral, topographic and functional connectivity analysis (www.github.com/BIAPT/EEGapp). Calculating functional connectivity on neurophysiological data typically requires neuroscientific and computational expertise, which presents a significant barrier to non-experts in both these domains. Our toolbox enables individuals without expertise in both fields to conduct these analyses on EEG collected from both wearable and research-grade systems. Computer scientists with limited medical expertise benefit from receiving the EEG data and all necessary accompanying information in a pre-defined MATLAB structure format – the output of the popular EEGLAB software package [45] – and clinicians with limited computing expertise benefit from a simple user interface which automates many sections of the analysis (e.g. comparison of functional connectivity against surrogate data) that are required to accurately interpret the results. Furthermore, the open-source nature of our toolbox allows the interested researcher to customize individual functions for their needs and to incorporate individual sections into larger analysis protocols.

Together with the open-source toolbox, the results of this study lay the groundwork for using EEG-based functional connectivity measures in non-laboratory and non-research settings. Functional connectivity changes recorded with research-grade EEG systems have been implicated in distinguishing loss and recovery of consciousness [27], [31], [40] and delirium [41]; the DSI-24 headset presents a high-quality wearable option for detecting these conditions in clinically-relevant settings (e.g. the intensive care unit, operating room). Functional connectivity patterns have also been used to identity changes associated with autism [42], dementia [43] and fragile X syndrome [44]; future applications of this current research can investigate the feasibility of using high-quality wearable systems to translate such findings to point-of-care diagnostic and assessment devices. While the findings of this study apply only to phase-based measures of functional connectivity and the quality of wearable EEG headsets based on other types (e.g. envelop-based) of connectivity remains an open-research question, it provides a strong template for evidence-based selection of the highest-quality system for collecting neurophysiological data in non-laboratory settings.

VI. CONCLUSION

Functional connectivity provides complementary information in the assessment of the quality of wearable EEG systems and can be used to generate more nuanced distinctions between otherwise-comparable systems. The inclusion of this metric in wearable EEG system assessment is further warranted by the increasing interest in brain connectivity in the neuroscientific community. We provide an EEG analysis toolbox that allows researchers and non-experts to explore spectral and functional connectivity properties of EEG in hopes that the translational neuroscientific community will be able to benefit from and contribute to these tools.

ACKNOWLEDGMENT

The authors would like to thank F. Tordini from CIRMMT for lending them two of the EEG headsets, as well as A. Johnson for his help with the OpenBCI.

REFERENCES

[1] *NeuroSky Body and Mind. Quantified*. Accessed: Sep. 25, 2020. [Online]. Available: http://neurosky.com/

[2] EMOTIV. *Emotiv—Leaders in Wireless EEG Brain Monitoring Technology*. Accessed: Sep. 25, 2020. [Online]. Available: https://www.emotiv.com/
[3] *XWave*. Accessed: Sep. 25, 2020. [Online]. Available: https://eyecomtec.com/3405-XWave/
[4] *NecoMimi Brainwave Cat Ears Review | Moving Cat Ears Headset*. Accessed: Sep. 25, 2020. [Online]. Available: https://www.necomimi.com/
[5] (Muse). *Muse—Meditation Made Easy.* Accessed: Sep. 25, 2020. [Online]. Available: https://choosemuse.com/
[6] *OpenBCI—Open Source Biosensing Tools (EEG, EMG, EKG, and More)*. Accessed: Sep. 25, 2020. [Online]. Available: https://openbci.com/?utm_source=google&utm_medium=cpc&utm_campaign=716348300&utm_content=open%20bci&gclid=Cj0KCQjwqrb7BRDlARIsACwGad53LV_cqhnpKhB9iS-5iXcUbys8E-CNrtLfEEdsvbdU2oYIa2oG3vYaAspTEALw_wcB
[7] P. Sawangjai, S. Hompoonsup, P. Leelaarporn, S. Kongwudhikunakorn, and T. Wilaiprasitporn, "Consumer grade EEG measuring sensors as research tools: A review," *IEEE Sensors J.*, vol. 20, no. 8, pp. 3996–4024, Apr. 2020, doi: 10.1109/JSEN.2019.2962874.
[8] W. O. Tatum, L. Winters, M. Gieron, E. A. Passaro, S. Benbadis, J. Ferreira, and J. Liporace, "Outpatient seizure identification: Results of 502 patients using computer-assisted ambulatory EEG," *J. Clin. Neurophysiol.*, vol. 18, no. 1, pp. 14–19, Jan. 2001.
[9] J. R. Wolpaw, "Brain-computer interfaces (BCIs) for communication and control: A mini-review," *Suppl. Clin. Neurophysiol.*, vol. 57, pp. 607–613, 2004.
[10] G. Borghini, L. Astolfi, G. Vecchiato, D. Mattia, and F. Babiloni, "Measuring neurophysiological signals in aircraft pilots and car drivers for the assessment of mental workload, fatigue and drowsiness," *Neurosci. Biobehavioral Rev.*, vol. 44, pp. 58–75, Jul. 2014, doi: 10.1016/j.neubiorev.2012.10.003.
[11] S. Makeig and M. Inlow, "Lapse in alertness: Coherence of fluctuations in performance and EEG spectrum," *Electroencephalogr. Clin. Neurophysiol.*, vol. 86, no. 1, pp. 23–35, Jan. 1993.
[12] T. Thompson, T. Steffert, T. Ros, J. Leach, and J. Gruzelier, "EEG applications for sport and performance," *Methods*, vol. 45, no. 4, pp. 279–288, Aug. 2008, doi: 10.1016/j.ymeth.2008.07.006.
[13] B. Hu, H. Peng, Q. Zhao, B. Hu, D. Majoe, F. Zheng, and P. Moore, "Signal quality assessment model for wearable EEG sensor on prediction of mental stress," *IEEE Trans. Nanobiosci.*, vol. 14, no. 5, pp. 553–561, Jul. 2015, doi: 10.1109/TNB.2015.2420576.
[14] J. Frey, "Comparison of an open-hardware electroencephalography amplifier with medical grade device in brain-computer interface applications," 2016, *arXiv:1606.02438*. [Online]. Available: http://arxiv.org/abs/1606.02438
[15] O. E. Krigolson, C. C. Williams, A. Norton, C. D. Hassall, and F. L. Colino, "Choosing MUSE: Validation of a low-cost, portable EEG system for ERP research," *Frontiers Neurosci.*, vol. 11, Mar. 2017, doi: 10.3389/fnins.2017.00109.
[16] M. P. Barham, G. M. Clark, M. J. Hayden, P. G. Enticott, R. Conduit, and J. A. G. Lum, "Acquiring research-grade ERPs on a shoestring budget: A comparison of a modified emotiv and commercial SynAmps EEG system: BARHAM et al.," *Psychophysiology*, vol. 54, no. 9, pp. 1393–1404, Sep. 2017, doi: 10.1111/psyp.12888.
[17] J. G. Cruz-Garza, J. A. Brantley, S. Nakagome, K. Kontson, M. Megjhani, D. Robleto, and J. L. Contreras-Vidal, "Deployment of mobile EEG technology in an art museum setting: Evaluation of signal quality and usability," *Frontiers Hum. Neurosci.*, vol. 11, Nov. 2017, doi: 10.3389/fnhum.2017.00527.
[18] J. J. Halford, R. J. Schalkoff, K. E. Satterfield, G. U. Martz, E. Kutluay, C. G. Waters, and B. C. Dean, "Comparison of a novel dry electrode headset to standard routine EEG in veterans," *J. Clin. Neurophysiol.*, vol. 33, no. 6, pp. 530–537, Dec. 2016, doi: 10.1097/WNP.0000000000000284.
[19] L. Mayaud, M. Congedo, A. Van Laghenhove, D. Orlikowski, M. Figère, E. Azabou, and F. Cheliout-Heraut, "A comparison of recording modalities of P300 event-related potentials (ERP) for brain-computer interface (BCI) paradigm," *Neurophysiologie Clinique/Clin. Neurophysiol.*, vol. 43, no. 4, pp. 217–227, Oct. 2013, doi: 10.1016/j.neucli.2013.06.002.
[20] T. Radntz, "Signal quality evaluation of emerging EEG devices," *Frontiers Physiol.*, vol. 9, p. 98, Feb. 2018, doi: 10.3389/fphys.2018.00098.
[21] T. S. Grummett, R. E. Leibbrandt, T. W. Lewis, D. DeLosAngeles, D. M. W. Powers, J. O. Willoughby, K. J. Pope, and S. P. Fitzgibbon, "Measurement of neural signals from inexpensive, wireless and dry EEG systems," *Physiological Meas.*, vol. 36, no. 7, pp. 1469–1484, Jul. 2015, doi: 10.1088/0967-3334/36/7/1469.
[22] S. Debener, F. Minow, R. Emkes, K. Gandras, and M. de Vos, "How about taking a low-cost, small, and wireless EEG for a walk: EEG to go," *Psychophysiology*, vol. 49, no. 11, pp. 1617–1621, Nov. 2012, doi: 10.1111/j.1469-8986.2012.01471.x.
[23] C. Guger, G. Krausz, B. Z. Allison, and G. Edlinger, "Comparison of dry and gel based electrodes for P300 brain–computer interfaces," *Frontiers Neurosci.*, vol. 6, p. 60, 2012, doi: 10.3389/fnins.2012.00060.
[24] K. J. Friston, "Functional and effective connectivity: A review," *Brain Connectivity*, vol. 1, no. 1, pp. 13–36, Jan. 2011, doi: 10.1089/brain.2011.0008.
[25] P. Boveroux, A. Vanhaudenhuyse, M.-A. Bruno, Q. Noirhomme, S. Lauwick, A. Luxen, C. Degueldre, A. Plenevaux, C. Schnakers, C. Phillips, J.-F. Brichant, V. Bonhomme, P. Maquet, M. D. Greicius, S. Laureys, and M. Boly, "Breakdown of within- and between-network resting state functional magnetic resonance imaging connectivity during propofol-induced loss of consciousness," *Anesthesiology*, vol. 113, no. 5, pp. 1038–1053, Nov. 2010, doi: 10.1097/ALN.0b013e3181f697f5.
[26] D. Jordan, R. Ilg, V. Riedl, A. Schorer, S. Grimberg, S. Neufang, A. Omerovic, S. Berger, G. Untergehrer, C. Preibisch, E. Schulz, T. Schuster, M. Schröter, V. Spoormaker, C. Zimmer, B. Hemmer, A. Wohlschläger, E. F. Kochs, and G. Schneider, "Simultaneous electroencephalographic and functional magnetic resonance imaging indicate impaired cortical top–down processing in association with anesthetic-induced unconsciousness," *Anesthesiology*, vol. 119, no. 5, pp. 1031–1042, Nov. 2013, doi: 10.1097/ALN.0b013e3182a7ca92.
[27] U. Lee, S. Ku, G. Noh, S. Baek, B. Choi, and G. A. Mashour, "Disruption of frontal-parietal communication by ketamine, propofol, and sevoflurane," *J. Amer. Soc. Anesthesiologists*, vol. 118, no. 6, pp. 1264–1275, 2013.
[28] A. Ranft, D. Golkowski, T. Kiel, V. Riedl, P. Kohl, G. Rohrer, J. Pientka, S. Berger, A. Thul, M. Maurer, C. Preibisch, C. Zimmer, G. A. Mashour, E. F. Kochs, D. Jordan, and R. Ilg, "Neural correlates of sevoflurane-induced unconsciousness identified by simultaneous functional magnetic resonance imaging and electroencephalography," *Anesthesiology*, vol. 125, no. 5, pp. 861–872, Nov. 2016, doi: 10.1097/ALN.0000000000001322.
[29] F. Agosta, E. Canu, P. Valsasina, N. Riva, A. Prelle, G. Comi, and M. Filippi, "Divergent brain network connectivity in amyotrophic lateral sclerosis," *Neurobiol. Aging*, vol. 34, no. 2, pp. 419–427, Feb. 2013, doi: 10.1016/j.neurobiolaging.2012.04.015.
[30] A. F. Alexander-Bloch, N. Gogtay, D. Meunier, R. Birn, L. Clasen, F. Lalonde, R. Lenroot, J. Giedd, and E. T. Bullmore, "Disrupted modularity and local connectivity of brain functional networks in childhood-onset schizophrenia," *Frontiers Syst. Neurosci.*, vol. 4, p. 147, 2010, doi: 10.3389/fnsys.2010.00147.
[31] H. Lee, G. A. Mashour, G.-J. Noh, S. Kim, and U. Lee, "Reconfiguration of network hub structure after propofol-induced unconsciousness," *Anesthesiology*, vol. 119, no. 6, pp. 1347–1359, Dec. 2013, doi: 10.1097/ALN.0b013e3182a8ec8c.
[32] V. I. Spoormaker, M. S. Schroter, P. M. Gleiser, K. C. Andrade, M. Dresler, R. Wehrle, P. G. Samann, and M. Czisch, "Development of a large-scale functional brain network during human non-rapid eye movement sleep," *J. Neurosci.*, vol. 30, no. 34, pp. 11379–11387, Aug. 2010, doi: 10.1523/JNEUROSCI.2015-10.2010.
[33] A. K. Engel, C. Gerloff, C. C. Hilgetag, and G. Nolte, "Intrinsic coupling modes: Multiscale interactions in ongoing brain activity," *Neuron*, vol. 80, no. 4, pp. 867–886, Nov. 2013, doi: 10.1016/j.neuron.2013.09.038.
[34] M. Siegel, T. H. Donner, and A. K. Engel, "Spectral fingerprints of large-scale neuronal interactions," *Nature Rev. Neurosci.*, vol. 13, no. 2, pp. 121–134, Feb. 2012, doi: 10.1038/nrn3137.
[35] L. Astolfi, F. Cincotti, D. Mattia, M. G. Marciani, L. A. Baccala, F. D. V. Fallani, S. Salinari, M. Ursino, M. Zavaglia, and F. Babiloni, "Assessing cortical functional connectivity by partial directed coherence: Simulations and application to real data," *IEEE Trans. Biomed. Eng.*, vol. 53, no. 9, pp. 1802–1812, Sep. 2006, doi: 10.1109/TBME.2006.873692.
[36] L. Astolfi, F. Cincotti, D. Mattia, C. Babiloni, F. Carducci, A. Basilisco, P. M. Rossini, S. Salinari, L. Ding, Y. Ni, B. He, and F. Babiloni, "Assessing cortical functional connectivity by linear inverse estimation and directed transfer function: Simulations and application to real data," *Clin. Neurophysiol.*, vol. 116, no. 4, pp. 920–932, Apr. 2005, doi: 10.1016/j.clinph.2004.10.012.

[37] K. Friston, R. Moran, and A. K. Seth, "Analysing connectivity with granger causality and dynamic causal modelling," *Current Opinion Neurobiol.*, vol. 23, no. 2, pp. 172–178, Apr. 2013, doi: 10.1016/j.conb.2012.11.010.
[38] M. Staniek and K. Lehnertz, "Symbolic transfer entropy," *Phys. Rev. Lett.*, vol. 100, no. 15, Apr. 2008, Art. no. 158101.
[39] C. J. Stam and E. C. W. van Straaten, "Go with the flow: Use of a directed phase lag index (dPLI) to characterize patterns of phase relations in a large-scale model of brain dynamics," *NeuroImage*, vol. 62, no. 3, pp. 1415–1428, Sep. 2012, doi: 10.1016/j.neuroimage.2012.05.050.
[40] S. Blain-Moraes, U. Lee, S. Ku, G. Noh, and G. A. Mashour, "Electroencephalographic effects of ketamine on power, cross-frequency coupling, and connectivity in the alpha bandwidth," *Frontiers Syst. Neurosci.*, vol. 8, p. 114, Jul. 2014, doi: 10.3389/fnsys.2014.00114.
[41] E. van Dellen, A. W. van der Kooi, T. Numan, H. L. Koek, F. A. M. Klijn, M. P. Buijsrogge, C. J. Stam, and A. J. C. Slooter, "Decreased functional connectivity and disturbed directionality of information flow in the electroencephalography of intensive care unit patients with delirium after cardiac surgery," *Anesthesiology*, vol. 121, no. 2, pp. 328–335, Aug. 2014, doi: 10.1097/ALN.0000000000000329.
[42] M. Boersma, C. Kemner, M. A. de Reus, G. Collin, T. M. Snijders, D. Hofman, J. K. Buitelaar, C. J. Stam, and M. P. van den Heuvel, "Disrupted functional brain networks in autistic toddlers," *Brain Connectivity*, vol. 3, no. 1, pp. 41–49, Feb. 2013, doi: 10.1089/brain.2012.0127.
[43] E. C. W. van Straaten, J. den Haan, H. de Waal, W. M. van der Flier, F. Barkhof, N. D. Prins, and C. J. Stam, "Disturbed phase relations in white matter hyperintensity based vascular dementia: An EEG directed connectivity study," *Clin. Neurophysiol.*, vol. 126, no. 3, pp. 497–504, Mar. 2015, doi: 10.1016/j.clinph.2014.05.018.
[44] M. J. W. van der Molen, C. J. Stam, and M. W. van der Molen, "Resting-state EEG oscillatory dynamics in fragile X syndrome: Abnormal functional connectivity and brain network organization," *PLoS ONE*, vol. 9, no. 2, p. e88451, Feb. 2014, doi: 10.1371/journal.pone.0088451.
[45] A. Delorme and S. Makeig, "EEGLAB: An open source toolbox for analysis of single-trial EEG dynamics including independent component analysis," *J. Neurosci. Methods*, vol. 134, no. 1, pp. 9–21, Mar. 2004, doi: 10.1016/j.jneumeth.2003.10.009.
[46] C. J. Stam, G. Nolte, and A. Daffertshofer, "Phase lag index: Assessment of functional connectivity from multi channel EEG and MEG with diminished bias from common sources," *Hum. Brain Mapping*, vol. 28, no. 11, pp. 1178–1193, Nov. 2007, doi: 10.1002/hbm.20346.
[47] J. Shin, G. A. Mashour, S. Ku, S. Kim, and U. Lee, "Subgraph 'backbone' analysis of dynamic brain networks during consciousness and anesthesia," *PLoS ONE*, vol. 8, no. 8, Aug. 2013, Art. no. e70899, doi: 10.1371/journal.pone.0070899.
[48] S. W. Hughes and V. Crunelli, "Thalamic mechanisms of EEG alpha rhythms and their pathological implications," *Neuroscientist*, vol. 11, no. 4, pp. 357–372, Aug. 2005, doi: 10.1177/1073858405277450.
[49] S. Blain-Moraes, V. Tarnal, G. Vanini, T. Bel-Behar, E. Janke, P. Picton, G. Golmirzaie, B. J. A. Palanca, M. S. Avidan, M. B. Kelz, and G. A. Mashour, "Network efficiency and posterior alpha patterns are markers of recovery from general anesthesia: A high-density electroencephalography study in healthy volunteers," *Frontiers Human Neurosci.*, vol. 11, Jun. 2017, doi: 10.3389/fnhum.2017.00328.
[50] H. Berger, "Uber das Elektrenkephalogramm des Menschen II," *J. Psychol. Neurol.*, vol. 40, pp. 160–179, Dec. 1930.
[51] R. L. Cannon, H. E. Pigott, T. Surmeli, D. R. Simkin, R. W. Thatcher, W. Van den Bergh, G. Gluck, J. F. Lubar, R. Davis, D. S. Foster, J. Douglas, A. T. Malcolm, D. Bars, K. Little, W. Center, M. Berman, H. Russell, B. Hammer, and J. L. Koberda, "The problem of patient heterogeneity and lack of proper training in a study of EEG neurofeedback in children," *J. Clin. Psychiatry*, vol. 75, no. 3, pp. 289–290, Mar. 2014, doi: 10.4088/JCP.13lr08850.
[52] D. C. Hammond, "The need for individualization in neurofeedback: heterogeneity in QEEG patterns associated with diagnoses and symptoms," *Appl. Psychophysiol. Biofeedback*, vol. 35, no. 1, p. 31, Sep. 2009, doi: 10.1007/s10484-009-9106-1.
[53] S. K. Loo and S. Makeig, "Clinical utility of EEG in attention-deficit/hyperactivity disorder: A research update," *Neurotherapeutics*, vol. 9, no. 3, pp. 569–587, Jul. 2012, doi: 10.1007/s13311-012-0131-z.

YACINE MAHDID received the B.Sc. degree in neuroscience with a minor in computer science from McGill University, Montreal, Canada, in 2017, where he is currently pursuing the Ph.D. degree in neuroscience.

His research interests include applying machine learning techniques to neuroscience data to develop practical systems for individuals with disabilities, and to gain insight of the neural correlates of subjective experiences.

UNCHEOL LEE received the Ph.D. degree in physics from Postech University, South Korea, focusing on nonlinear dynamics and complex time series analysis of physiological data.

He was a Postdoctoral Fellow with the Max Plank Institute for Physics for complex systems, and worked as a Visiting Scholar with the Asian Pacific Center for Theoretical Physics, South Korea. Since 2014, he has been an Assistant Professor with the Department of Anesthesiology, University of Michigan. He is the author of over 50 articles. He is the Associate Director of the Center for Consciousness Science. His research interests include the study the dynamics of brain networks and connectivity, specifically in mathematical, and computational model studies of the brain.

STEFANIE BLAIN-MORAES received the B.A.Sc. degree in engineering science from the University of Toronto, in 2005, and the Ph.D. degree in biomedical engineering and rehabilitation sciences from the University of Toronto, in 2010.

From 2010 to 2015, she was a Postdoctoral Fellow with the University of Michigan. Since 2016, she has been an Assistant Professor with the School of Physical and Occupational Therapy, McGill University. She is the author of over 40 journal articles and over 40 conference contributions. Her research interests include the assessment of consciousness in non-communicative individuals and the development of assistive technologies to interact with those who are behaviorally unresponsive.

Dr. Blain-Moraes was selected in 2017 by the World Economic Forum as one of 50 extraordinary scientists under the age of 40 to participate in the Annual Meeting of the New Champions, and is the Canada Research Chair (Tier II) of Consciousness and Personhood Technology.